Fuel Processing Session II: Catalysis and Kinetics

Characterization of PROX Catalysts on Structured Supports

Paul Chin, George W. Roberts, Xiaolei Sun[1], and James J. Spivey[2]*

North Carolina State University
Department of Chemical Engineering, Box 7905
Ralei gh, NC 27695-7905

[1] – Current Address: Akzo-Nobel Chemicals Research
1 Livingstone Ave.
Dobbs Ferry, NY 10522-3401

[2] – Current Address: Louisiana State University
Department of Chemical Engineering
Baton Rouge, LA 70803

* - Corresponding Author:
E-mail: groberts@eos.ncsu.edu
Telephone: (919) 515-7328
Fax: (919) 515-3465

Introduction:

The study of carbon monoxide removal in the presence of a hydrogen-rich gas stream is well-established. Traditional methods use CO hydrogenation or pressure-swing adsorption to remove the undesired CO. An alternative method for CO removal is oxidation. In the presence of oxygen, the catalyst must actively and selectively oxidize CO instead of H_2.

The development of practical fuel cell power for both automotive transportation and stationary applications requires the manufacture of fuel processors that convert liquid fuels into H_2 and carbon dioxide [1-3]. Fuel processors must be compact, mechanically durable, quick-starting, responsive to transient demands, and inexpensive. Proton-exchange membrane fuel cells (PEMFCs) have been specifically targeted for automotive applications because of their high power density and low operating temperatures [1-6]. The inlet gas feed for the PEMFC must have very low CO concentrations to avoid poisoning the Pt electrodes [1-9].

The final oxidation step prior to the PEMFC requires an active catalyst for CO oxidation (reaction R1) to reduce the CO concentration from ~1% to less than 10 ppm in the presence of high H_2, CO_2, and steam concentrations, using a minimum weight and volume of catalyst. However, the catalyst must not oxidize a significant quantity of H_2 (reaction R2) since it is the fuel used in the PEMFC anode. Any H_2 consumed by reaction R2 during the selective oxidation step must be replaced, increasing both the size of, and the rate of feed to, the fuel processor. Therefore, the catalyst must be highly active and selective for CO oxidation over H_2. This process is known as "preferential oxidation" in the fuel cell community, and is referred to as the acronym "PROX."

$$CO + \tfrac{1}{2}O_2 \rightarrow CO_2 \qquad (\Delta H_{rxn,298K} = -283 \text{ kJ/mol}) \qquad \text{R1}$$

$$H_2 + \tfrac{1}{2}O_2 \rightarrow H_2O \qquad (\Delta H_{rxn,298K} = -242 \text{ kJ/mol}) \qquad \text{R2}$$

$$CO_2 + H_2 \rightleftarrows CO + H_2O \qquad (\Delta H_{rxn,298K} = +41.2 \text{ kJ/mol}) \qquad \text{R3}$$

Thermodynamically, CO oxidation is more favorable than H_2 oxidation ($\Delta G_{rxn,298K}$ = -257 kJ/mol versus -229 kJ/mol, respectively), and evolves more heat, as seen in the $\Delta H_{rxn,298K}$ for reactions R1 and R2. Based on the exothermic nature of these two reactions, some commercial designs for this element of the fuel processor use two fixed-bed adiabatic reactors in series, with an intermediate cooling step [10]. Adiabatic reactors may not be the ideal reactor design because the reverse water-gas-shift (r-WGS, reaction R3) reaction is favored by higher temperatures ($\Delta G_{rxn,298K}$ = +28.6 kJ/mol). This side reaction can prevent the PROX reactor from reaching low CO concentrations [11-15]. For typical PROX gas compositions, the gas temperature increases by about 90°C for every 0.5% of O_2 that is reacted, if the PROX reactor is operated adiabatically.

Many of the PROX catalysts that have been reported in the open literature have been prepared on high surface area (> 100 m^2/g) particulate supports. At least one group of investigators has evaluated low surface area (< 25 m^2/g) particulates [16]. Finned metallic

surfaces [9, 17] and ceramic monoliths [11, 18] also have received some attention. In addition, effective PROX catalysts have been synthesized on metal foams [19].

Experimental:

An Fe-promoted Pt catalyst was synthesized on a ceramic, straight-channel monolith with 400 cells per square inch (cpsi). The cells had square cross sections. The surface area per unit volume for this support was about 2.8 mm^{-1}. An Al_2O_3 washcoat was applied to the monolith with a loading of 1.6 g/in^3 of gross catalyst volume. Assuming a dry washcoat density of 2.0 gr/cm^3, the calculated average thickness of the washcoat was approximately 15 to 20 μm. The Pt concentration was 5 wt.%, based on the amount of washcoat, and the Fe concentration was 0-1 wt.%, again based on the amount of washcoat.

Each piece of catalyst had an outer diameter of 1 inch and was 2 inches in length. The catalysts were wrapped with ceramic insulation and fitted into a stainless-steel tube with an inside diameter of 1.125 inches. The reactor was operated close to adiabatic conditions by wrapping the stainless-steel tube with an inner layer of ceramic blanket insulation. Heating tape was then wrapped around the inner insulation layer, and an outer insulation layer was wrapped over the heating tape. The concentration of CO in the reactor feed and the reactor effluent was measured using an on-line nondispersive infrared (NDIR) gas analyzer. The feed and effluent O_2 concentrations were measured with a paramagnetic analyzer. Both analyzers were provided by California Analytical Instruments, Inc. The CAI Model 300 analyzer includes two CO analyzers and one O_2 analyzer.

The catalyst was evaluated using the following gas composition: H_2 – 42%, CO_2 – 9%, H_2O – 12%, CO – 1.0%, O_2 – 0.50%, and N_2 – 35.5%. This composition simulates the gas that leaves the last water-gas-shift (WGS) reactor in a typical fuel processor. All experiments were conducted at a fixed reactor pressure of 2 atm (absolute). The inlet temperature was studied over the range from 100°C to 170ºC. The gas hourly space velocity (GHSV) was studied at 30,000 hr^{-1}. The space velocity was calculated by dividing the volumetric gas flow rate at standard conditions (1 atm; 21.1 °C) by the gross catalyst volume. The CO conversion (X_{CO}), CO selectivity (S_{CO}), and O_2 conversion (X_{O2}) were used to indicate catalyst performance. The CO selectivity was calculated as follows:

$$\text{CO Selectivity (\%)} = \frac{(\text{Inlet CO Concentration-Outlet CO Concentration})*100}{2*(\text{Inlet } O_2 \text{ Concentration - Outlet } O_2 \text{ Concentration})}$$

Results and Discussion:

Figure 1 shows the catalyst performance at 100°C inlet temperature, 1% CO inlet concentration, O_2/CO ratio = 1.0, and 30,000 hr^{-1} GHSV. At these conditions, there were distinct differences in the CO conversion and selectivity. At lower Fe loadings (0 and 0.05 wt% Fe), the CO conversion was less than 40% and the O_2 conversion was less than 30%. At higher Fe loadings (0.5 and 1.0 wt% Fe), the activity of the catalysts increased significantly; CO conversion was ~80%, and O_2 conversion was ~100%. Since the reactor is adiabatic, it is

uncertain whether the higher activity is because of an increased Fe loading or because of an increased reactor temperature.

It is impossible measure the true kinetic CO selectivity above the stoichiometric O_2/CO ratio over certain O_2 conversions. At an O_2/CO ratio = 1.0, the O_2 conversions for the lower 0 and 0.05 wt% Fe promoted catalysts measured the true kinetic CO selectivity of 62% and 98%, respectively. The higher 0.5 and 1.0 wt% Fe promoted catalysts did not measure the true kinetic CO selectivity because the O_2 conversions were too high (> 50%).

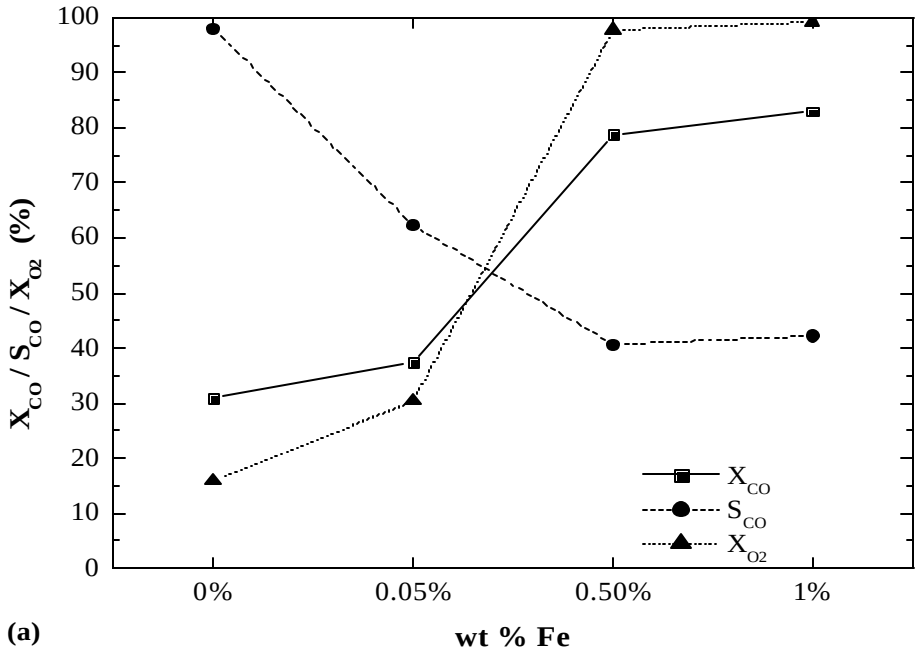

Figure 1: Effect of Fe weight loading on 400 cpsi, 5 wt% Pt / γ-Al_2O_3 ceramic straight-channel monoliths (1% CO inlet concentration, O_2/CO ratio = 1.0, GHSV = 30,000 hr^{-1}, T_{inlet} = 100°C)

Using typical gas stream compositions exiting the WGS reactor, the r-WGS reaction could severely limit CO conversion [11-13]. Limitations caused by the r-WGS reaction can be significant at higher temperatures (i.e. > 150°C), where the oxidation catalyst is moderately active and the r-WGS equilibrium favors CO formation.

Carbon monoxide was removed from the inlet stream to test the catalysts' activity for the r-WGS reaction. Under this condition, any CO detected in the outlet stream could be attributed to the r-WGS reaction (reaction R3). A r-WGS equilibrium curve was computed by a theoretical model with the following five assumptions: 1) No CO was in the inlet gas stream; 2) Hydrogen oxidation consumed all of the O_2; 3) The r-WGS reaction reached equilibrium at the outlet temperature; 4) The ideal gas law (PV=nRT) was valid; 5) The C_p's and ΔH_{rxn} were constant over a given range of temperatures.

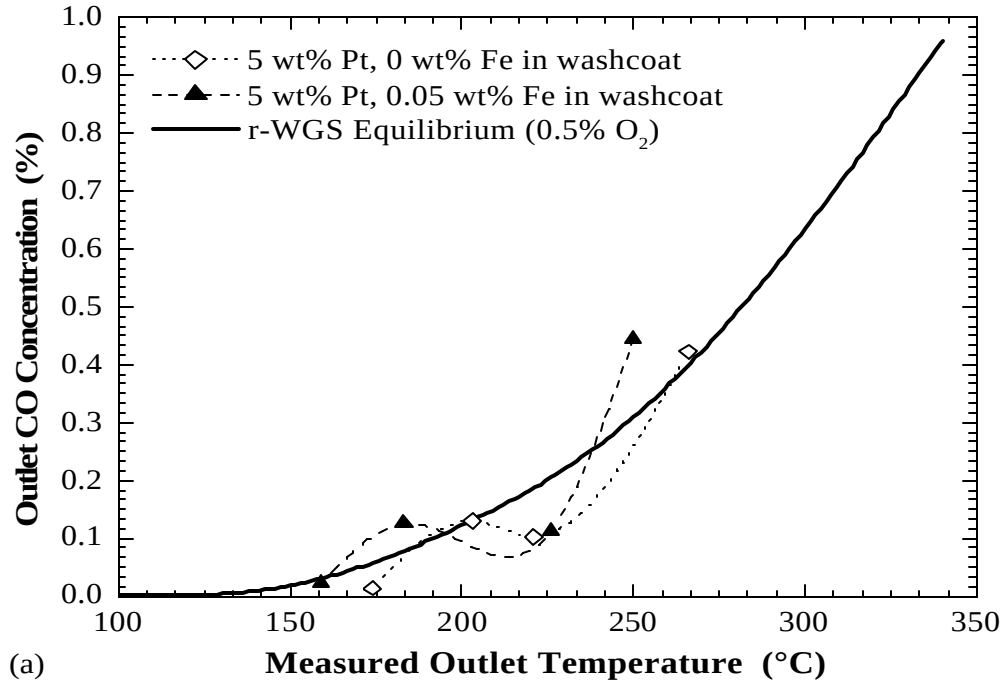

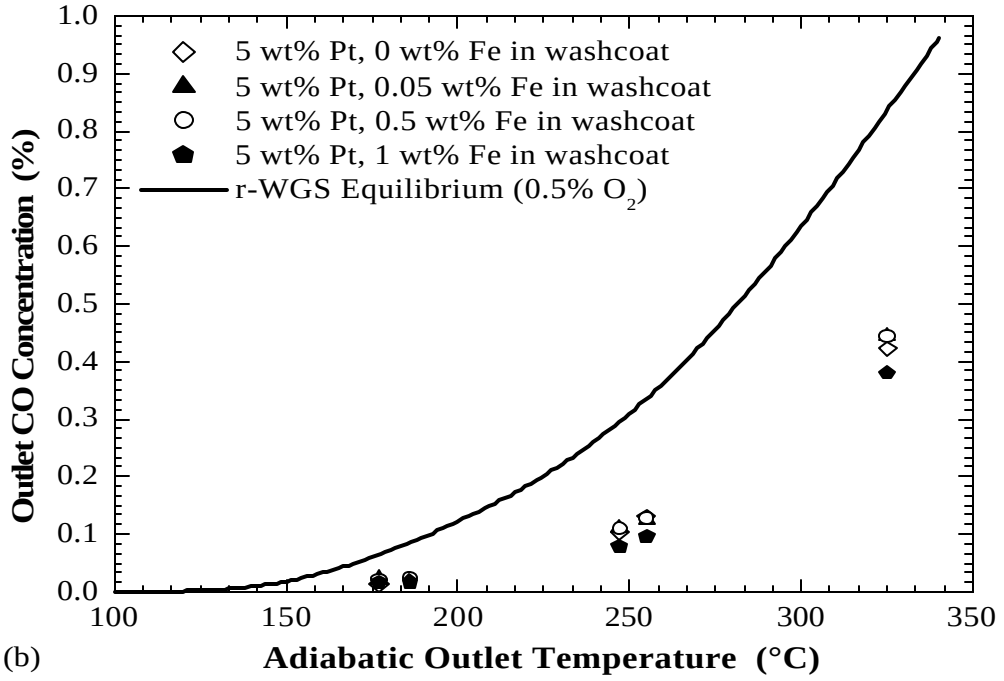

Figure 2: CO formed by the r-WGS reaction on 5 wt% Pt / 0-1 wt% Fe / γ-Al_2O_3 ceramic straight-channel monoliths as a function of (a) the measured outlet temperature and (b) the adiabatic reaction outlet temperature (no CO in the feed, varying O_2 concentration and/or inlet temperature, GHSV=30,000 hr^{-1})

The r-WGS equilibrium, shown as the solid line in Figure 2a, could limit the minimum outlet CO concentration exiting the PROX reactor under these conditions. Figure 2a shows the outlet CO concentration as a function of the measured reactor outlet temperature for the

5 wt% Pt / 0 & 0.05 wt% Fe / γ-Al_2O_3 ceramic straight-channel monoliths at different O_2 inlet concentrations and/or inlet temperatures. The 5 wt% Pt / 0.5 & 1.0 wt% Fe / γ-Al_2O_3 ceramic monolith data was not graphed, but exhibited a similar behavior.

The two catalysts shown in Figure 2a were active WGS catalysts because they approached, and in some cases exceeded, the r-WGS equilibrium. No correlation between the measured outlet temperature and the approach to the r-WGS equilibrium could be determined from this graph. The second and fourth outlet CO concentration points were above the predicted r-WGS equilibrium curve, while first and third data points were below, causing a decrease in outlet CO concentration from the second to third point albeit the increased outlet temperature. An explanation for this anomaly is transport limitations in the support, causing a temperature gradient between the catalyst surface and the bulk gas. The CO and H_2 oxidation reactions are very exothermic; if the heat transfer coefficient h_i between the catalyst surface and the bulk gas is small, then the catalyst surface temperature will exceed the measured bulk gas temperature, especially at high H_2 concentrations.

When the catalyst surface temperature is higher than the measured bulk gas temperature, the r-WGS reaction can equilibrate at a higher temperature than the measured bulk outlet temperature and increase the outlet CO concentration. This shift in the equilibrium is one explanation of why several outlet CO concentrations in Figure 2a are above the r-WGS equilibrium curve. Moreover, the location of the "hot spot" in the support affects the extent of the equilibrium shift. If the "hot spot" is located towards the inlet region of the catalyst, then the r-WGS reaction can re-equilibrate to a lower temperature in the latter portion of the catalyst before leaving the reactor. If the "hot spot" is located towards the outlet region of the catalyst, then the r-WGS reaction may not re-equilibrate to a lower outlet CO concentration.

Figure 2b is a re-plot of the data in Figure 2a with two differences: 1) the abscissa is the adiabatic reaction temperature instead of the measured outlet temperature, and 2) all the 5 wt% Pt / varying wt% Fe data is graphed. The adiabatic reaction temperature was calculated assuming 100% O_2 conversion. Every data point fell below the r-WGS equilibrium curve. In addition, the outlet CO concentration for each catalyst increased monotonically with the adiabatic outlet temperature. No obvious relationship between the Fe weight loading and the outlet CO concentration formed by the r-WGS reaction was discerned from Figure 2b. Even without the presence of Fe, the unpromoted Pt catalyst was an active WGS catalyst because it approached the r-WGS equilibrium [12, 15, 20].

Carbon monoxide pulse chemisorption and temperature programmed desorption (TPD) were used to determine the number of active metal sites. These characterization techniques were utilized to explain the variations in activity and selectivity between the different catalyst samples. An elongated tail in the pulse chemisorption tests was attributed to CO adsorption on either the γ-Al_2O_3 washcoat or on surface impurities. The CO desorption temperature measured from TPD tests ranged from 215-250°C. The pulse chemisorption and TPD results did not adequately describe the catalyst performance results. Higher values of the

number of CO adsorbed on the metal surface did not correspond to higher CO conversions seen in the PROX reaction from higher wt% Fe catalysts.

Conclusions:

Four 5 wt% Pt, 400 cpsi ceramic straight-channel monolith catalysts were synthesized with different Fe loadings. At 100°C inlet temperature and using an adiabatic reactor, higher Fe loadings increased CO and O_2 conversions and decreased CO selectivity. Since the reactor is adiabatic, it is uncertain whether the higher conversions and lower selectivity were caused by an increased Fe loading or by an increased reactor temperature. For the 5 wt% Pt / 0-1 wt% Fe ceramic monoliths, the r-WGS reaction constituted a potential barrier to achieving ppm level outlet CO concentrations. The reactor must be maintained at low temperatures (< 150°C) to limit the significance of this reaction in a PROX system. One way to achieve this goal is running the reactor isothermally instead of adiabatically to sustain low outlet temperatures and to suppress the r-WGS reaction. Pulse chemisorption and TPD experiments were performed in an attempt to describe the CO conversions seen in the PROX reaction. Higher values of the number of CO adsorbed on the active metal sites did not correspond to higher CO conversions.

Acknowledgements:

The authors would like to thank Porvair Fuel Cell Technology and the United States Department of Energy, under Contract Number DE-FG-01NT41277, for funding of this research. The catalyst used in this research was prepared by Environex, Inc., Devon, PA.

Literature Cited:

1. Heck, R.M. and R.J. Farrauto, Applied Catalysis A - General, 2001. **221**(1-2): p. 443-457.
2. Heck, R.M., R.J. Farrauto, and S.T. Gulati, *Catalytic Air Pollution Control Commercial Technology*. 2nd Edition ed. 2002, New York, NY: John Wiley & Sons, Inc. 391.
3. Farrauto, R.J. and R.M. Heck, Catalysis Today, 2000. **55**(1-2): p. 179-187.
4. Divisek, J., H.F. Oetjen, V. Peinecke, V.M. Schmidt, and U. Stimming, Electrochimica Acta, 1998. **43**(24): p. 3811-3815.
5. Larminie, J. and A. Dicks, *Fuel Cell Systems Explained*. 2000, West Sussex, England: John Wiley & Sons, Ltd. 308.
6. Song, C.S., Catalysis Today, 2002. **77**(1-2): p. 17-49.
7. Rohland, B. and V. Plzak, Journal of Power Sources, 1999. **84**(2): p. 183-186.
8. Gotz, M. and H. Wendt, Electrochimica Acta, 1998. **43**(24): p. 3637-3644.
9. Dudfield, C.D., R. Chen, and P.L. Adcock, International Journal of Hydrogen Energy, 2001. **26**(7): p. 763-775.
10. Igarashi, H., H. Uchida, M. Suzuki, Y. Sasaki, and M. Watanabe, Applied Catalysis A - General, 1997. **159**(1-2): p. 159-169.
11. Korotkikh, O. and R. Farrauto, Catalysis Today, 2000. **62**(2-3): p. 249-254.
12. Oh, S.H. and R.M. Sinkevitch, Journal of Catalysis, 1993. **142**(1): p. 254-262.
13. Manasilp, A. and E. Gulari, Applied Catalysis B-Environmental, 2002. **37**(1): p. 17-25.
14. Kim, D.H. and M.S. Lim, Applied Catalysis a-General, 2002. **224**(1-2): p. 27-38.
15. Brown, M.L., A.W. Green, G. Cohn, and H.C. Andersen, Industrial and Engineering Chemistry, 1960. **52**(10): p. 841-844.
16. De Wild, P., M. Verhaak, and D. Bakker, *Catalysts For the Selective Oxidation of Carbon Monoxide in Hydrogen-Containing Gases*, in *World Intellectual Property Organization*. 2000, De Bruijn, L: Netherlands.
17. Dudfield, C.D., R. Chen, and P.L. Adcock, Journal of Power Sources, 2000. **86**(1-2): p. 214-222.
18. Roberts, G.W., P. Chin, X.L. Sun, and J.J. Spivey, Applied Catalysis B-Environmental, 2003. **46**(3): p. 601-611.
19. Chin, P., G.W. Roberts, and J.J. Spivey, *Preferential Oxidation of Carbon Monoxide on Structured Supports*, in *Chemical Engineering*. 2004, North Carolina State University: Raleigh, NC. p. 210.
20. Watanabe, M., H. Uchida, K. Ohkubo, and H. Igarashi, Applied Catalysis B-Environmental, 2003. **46**(3): p. 595-600.